WYDZIAŁ ODLEWNICTWA AGH
ODDZIAŁ KRAKOWSKI STOP
XXXIII KONFERENCJA NAUKOWA
z okazji Ogólnopolskiego Dnia Odlewnika 2009
Kraków, 11-12 grudnia 2009 r.

Janusz LELITO[1], Paweł ŻAK[1], Józef Szczepan SUCHY[1], Witold KRAJEWSKI[1], Lindsay GREER[2], Peter SCHUMACHER[3], Amir SHIRZADI[2], Beata GRACZ [1]

MICROSTRUCTURE ANALYSIS OF THE AZ91/SiC COMPOSITE

INTRODUCTION

Magnesium alloys and their composites have been attracting attention as an important lightweight material and are being utilized in the automobile and aerospace industries [1-4].

In terms of the reinforcement in magnesium-based composites, the SiC particles are extensively used because magnesium cannot form any stable carbide [5].

Keywords: AZ91 alloy, AZ91/SiC composite, Mg_2Si phase

EXPERIMENTAL PROCEDURE

Materials and processing

The AZ91 alloy was selected as the matrix for the composites. The chemical composition is shown in Table 1. The reinforcement particles are silicon carbide with an average diameter of 45 μm. Composite specimen with 0 and 5 wt.% of SiC particles were prepared using a liquid mixing and casting process.

Table 1

Chemical composition of AZ91 alloy

Chemical composition / %wt.							
Al	Zn	Mn	Fe	Be	Si	Cu	Ni
9.03	0.6	0.2	0.0026	0.0011	0.0023	0.0016	0.00062

---

[1] Dr Janusz LELITO,
- Department of Foundry Processes Engineering in Faculty of Foundry Engineering AGH
M.Sc. Paweł ŻAK,
- Department of Foundry Processes Engineering in Faculty of Foundry Engineering AGH
Prof. Józef Szczepan SUCHY,
- Department of Foundry Processes Engineering in Faculty of Foundry Engineering AGH
Prof. Witold KRAJEWSKI,
- Department of Foundry Processes Engineering in Faculty of Foundry Engineering AGH
M.Sc. Beata GRACZ,
- PhD Students of Faculty of Foundry Engineering AGH

[2] Prof. Lindsay GREER,
- Department of Materials Science and Metallurgy in University of Cambridge
Dr Amir SHIRZADI,
- Department of Materials Science and Metallurgy in University of Cambridge

[3] Prof. Peter SCHUMACHER,
- Department of Metallurgy in University of Leoben

Processing of the magnesium composites consisted of mixing pre-heated SiC particles with liquid magnesium melt stirring and mould casting. About 1 kg of composite melts was prepared in an electric resistance furnace using a steel crucible under a SF_6/CO_2 gas atmosphere. The molten composite were held at 700°C for 1 h, stirred for 2 min, and then cast at 700°C into a mold to produce plates of 100 x 100 x 15 mm. An un-reinforced AZ91 alloy was also cast at the same temperature (700°C).

Thermal analysis

For the thermal analysis of the AZ91 alloy and composite samples, cooling curves during solidification were obtained using a data acquisition system (Agilent) at a sampling rate of 5 data per second. A chromel-alumel (K-type) thermocouple positioned 50 mm from the bottom of the plate center, was used to monitoring temperature as the melt solidified.

Microstructural analysis

The as-cast plates were sectioned and polished before microstructural analysis using transmission electron microscopy (SEM) and X-ray diffraction (XRD) method.

RESULTS

Thermal analysis

Typical cooling curve for AZ91 alloy and AZ91/SiC composite are shown in Figure 1 and 2 respectively. In both cases two important regions in the curve are identified: (P) nucleation of primary magnesium phase and (E) eutectic reaction. The equilibrium phase for these alloys is the solid α-Mg solution, but during solidification a nonequilibrium eutectic (α-Mg - β-$Mg_{17}Al_{12}$) is also created and present in the un-reinforced AZ91 alloy and in the AZ91/SiC composite. For AZ91/SiC composite cooling rate, Fig. 2, shows a third region (M) in which an exothermic reaction occurred.

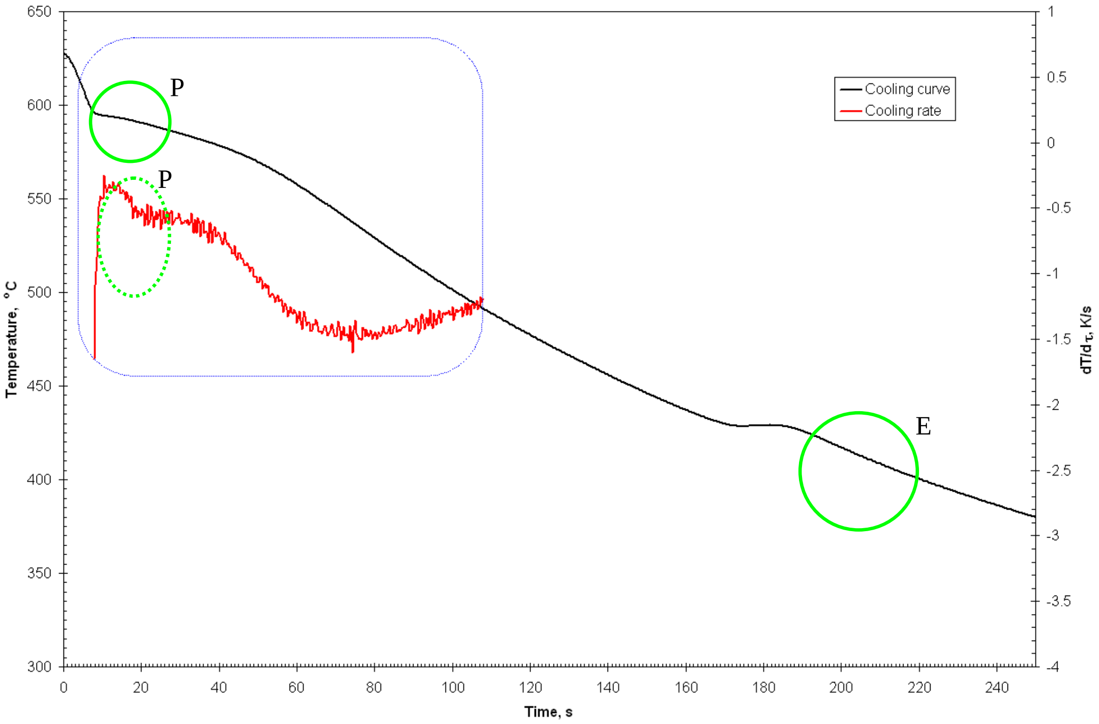

Fig. 1. Cooling curve and cooling rate of the AZ91 alloy

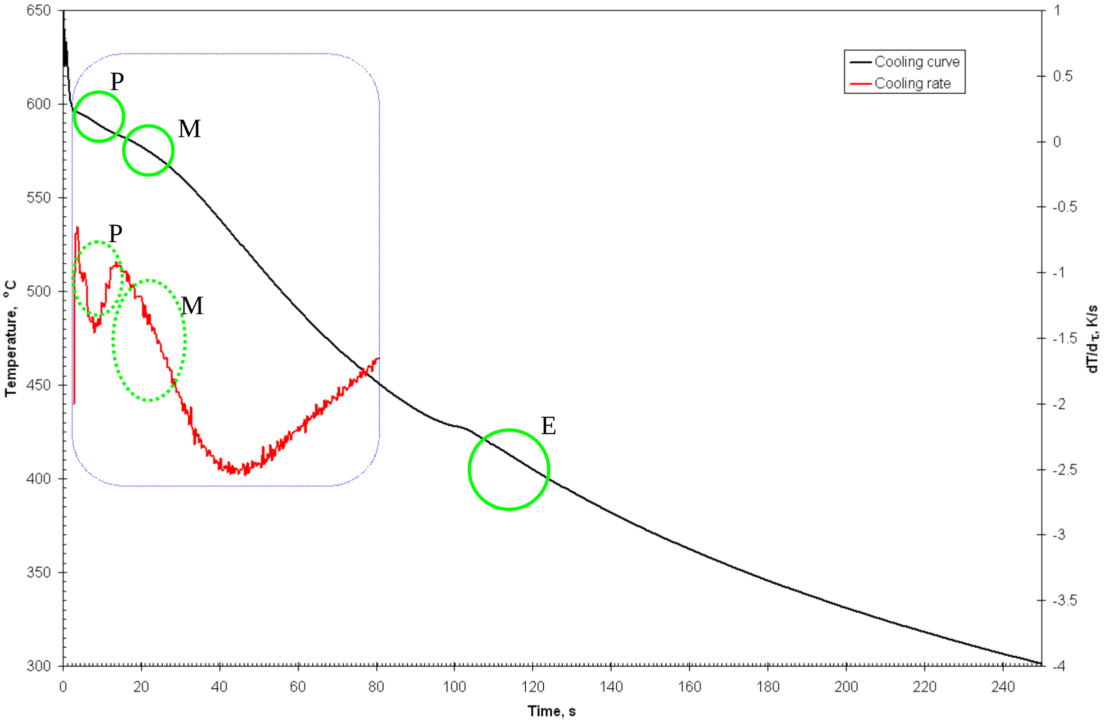

Fig. 2. Cooling curve and cooling rate of the AZ91/5wt.% SiC composite

Microstructural analysis

The X-ray diffraction examination of the AZ91 alloy (red line) and the composite (black line), Fig. 3, also confirmed the presence of the magnesium primary phase (α-Mg) and the β-$Mg_{17}(Al, Zn)_{12}$ phase in the microstructure. The XRD graph of the composite (black line in the Fig. 3) contains a peak about 24^{o} which shows the formation of intermetallic phase Mg_2Si.

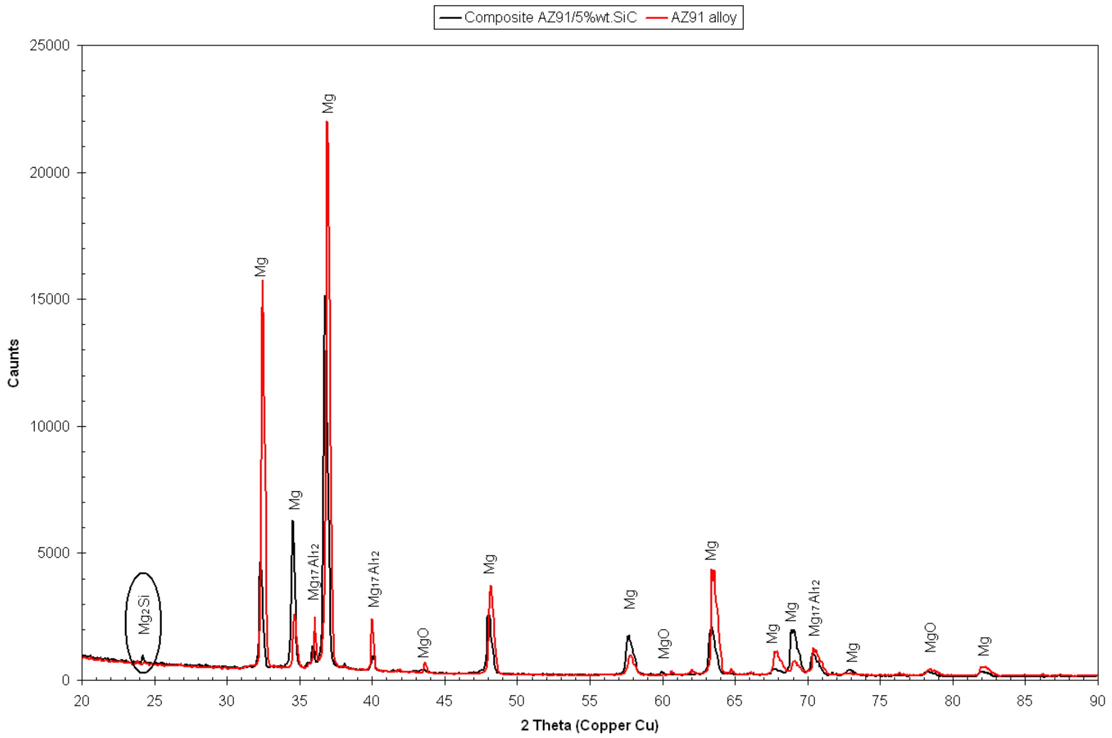

Fig. 3. The XRD graph of AZ91 alloy (red line) and composite reinforced 5 wt.% SiC (black line)

SEM examinations of the composite base on AZ91 5 wt.% SiC, Fig. 4 and 5, confirmed presence Mg_2Si phase in the microstructure. In addition to intermetallic phase Mg_2Si and SiC particles, another eutectic phase $Mg_{17}(Al, Zn)_{12}$ (grey area, Fig. 4 and blue area Fig. 5), primary phase Mg (dark matrix, Fig. 4 and green matrix, Fig 5) and AlMn phase (white points, Fig. 4 and 5) are also formed in the composite matrix. The analyses of chemical composition in area 1 of the precipitate (see Fig. 6), where approximately 39.443% of Al by weight and 51.689% of Mn by weight were found.

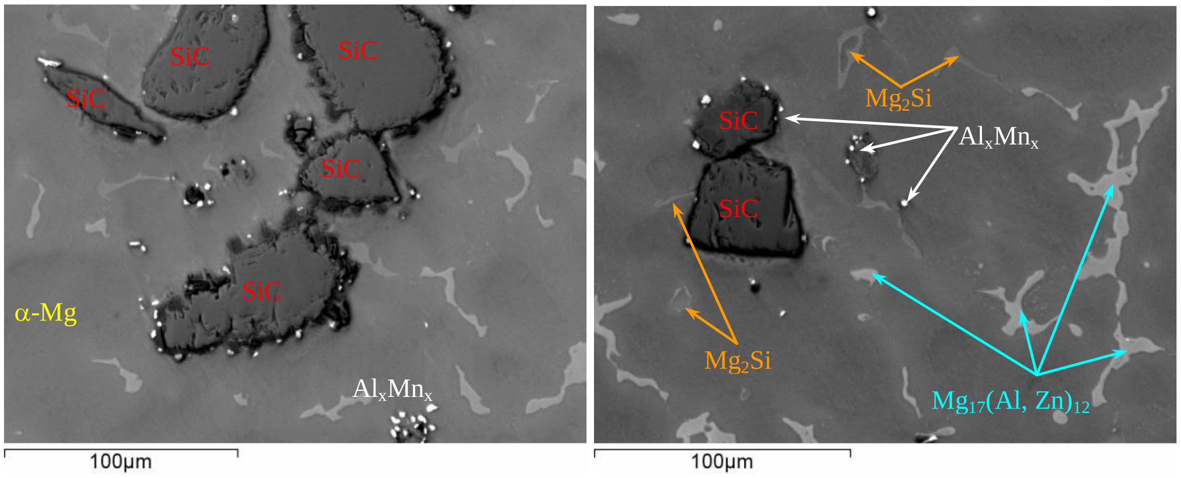

Fig. 4. SEM micrograph of the AZ91/SiC composite shows formation of Mg_2Si, AlMn, $Mg_{17}(Al, Zn)_{12}$, primary phase α-Mg and SiC particles

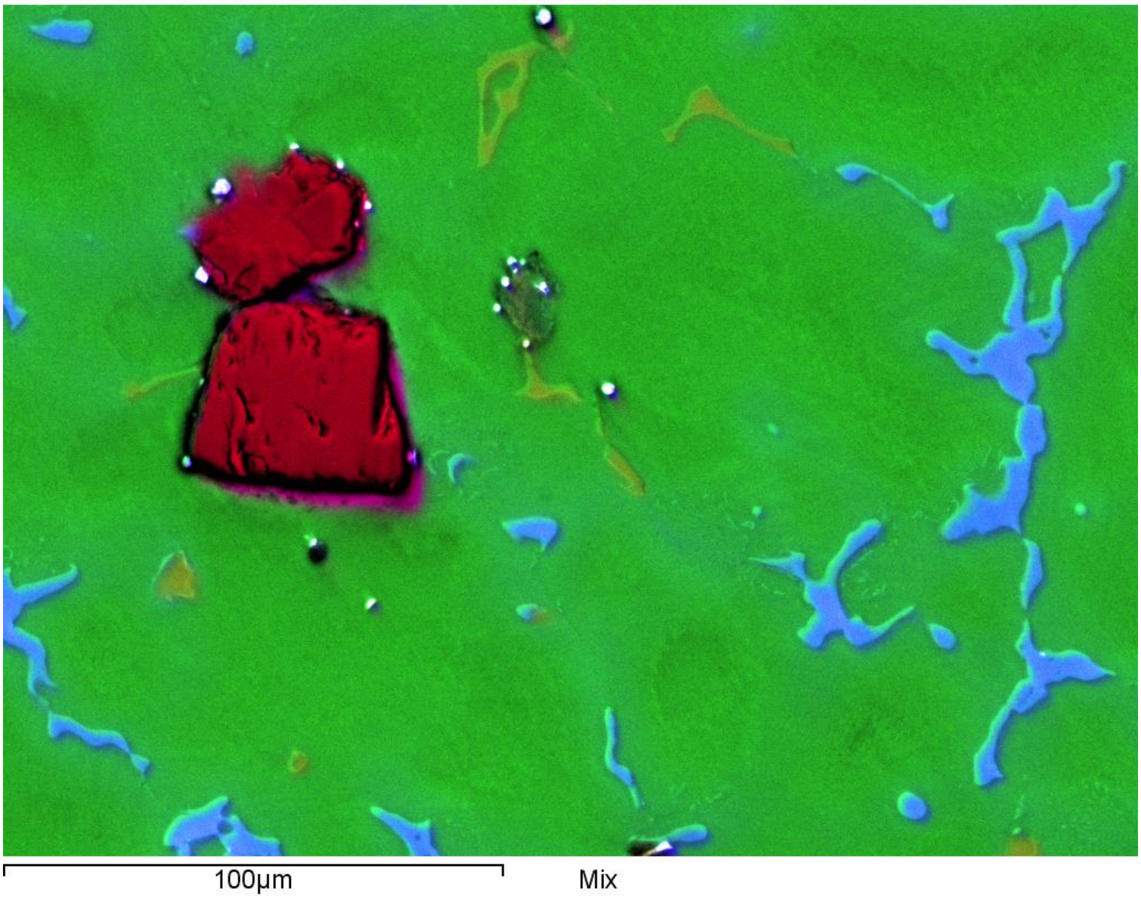

Si – Red Mg – Green Al – Blue Mn – white

Fig. 5. EDS map show distributions of various elements in AZ91/SiC composite

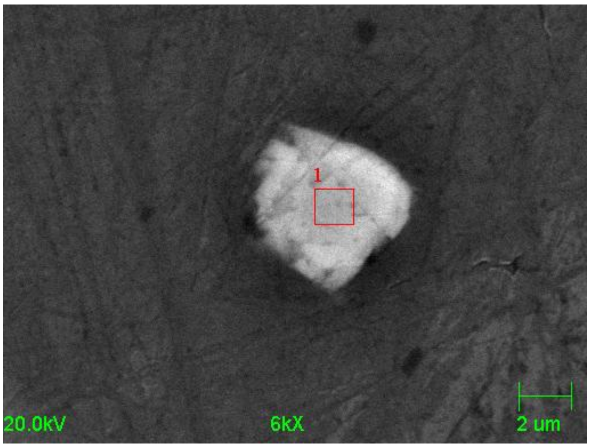

Fig. 6. SEM micrograph of the AZ91/SiC composite shows an AlMn precipitations within the matrix

SUMMARY AND DISCUSSION

The solidification process of the AZ91 alloy begins with the nucleation of the α-Mg primary phase dendrites. The α-Mg crystallite size is defined by several factors: self-cooling rate, chemical composition and the type of particles present in the liquid, which may serve as bases for heterogeneous nucleation.

It must be noted that during the crystallization of the primary phase dendrites the AlMn phase also crystallizes, which may serve as a base for heterogeneous nucleation of the α-Mg phase. The effect of the chemical composition on the crystallite size may be determined by the growth restriction coefficient.

The next phase of the AZ91 solidification is the crystallization of the eutectic, which itself is comprised of a mixture of the β-$Mg_{17}(Al, Zn)_{12}$ phase and the aluminum-rich α-Mg phase. The morphology of the eutectic and the liquid flow in the interdendritic areas may result in the growth of porosity.

The solidification process of the composite base on AZ91 alloy reinforced SiC particles occurs like solidification process of the AZ91 alloy un-reinforced SiC particles. Additionally, there appears the intermetalic phase Mg_2Si in the microstructure of the composite. Phase Mg_2Si exhibits a high melting temperature of 1085 ^{o}C, low density of 1.99x10^{3} kg m^{-3}, high hardness of 4.5x109 Nm^{-2}, a low thermal expansion coefficient of 7.5x10^{-6} K^{-1}, a reasonably high elastic modulus of 120 GPa [4] and binding energy between Mg and Si is very high (the enthalpy of formation is - 26.8 kJ per g-atom. Thus when small amounts of Si (for example 0.5 at %) are added to the alloy with 2 at % Mg, the 1 at % excess Mg would cause Mg_2Si [6]. Reactions between SiC, SiO_2 and Mg and Al might happen as follows:

$$\frac{1}{2}SiO_2 + Mg \rightarrow MgO + \frac{1}{2}Si \tag{1}$$

$$Mg + \frac{1}{2}Si \rightarrow \frac{1}{2}Mg_2Si \tag{2}$$

$$\frac{1}{2}SiC + Mg \rightarrow \frac{1}{2}Mg_2Si + \frac{1}{2}C \tag{3}$$

$$\frac{3}{4}SiC + Al \rightarrow \frac{1}{4}Al_4C_3 + \frac{3}{4}Si \tag{4}$$

These reactions depend on the processing parameters, especially on temperature and chemical composition of both the matrix and the reinforcement SiC particles. Authors [7] calculated the Gibbs free energies of reaction Eqs. (1) – (4) within the temperature range of 650–900 ^{o}C using thermodynamic data. The results indicate that there is no chemical reaction between SiC and magnesium, Eqs. (3), and between SiC and aluminum, Eqs. (4), at the temperature from 650 to 900 ^{o}C because the Gibbs free energies of reaction changes from 941 J to 4900 J for Eqs. (3) and from 5154 J to 9678 J for Eqs. (4). The Gibbs free energies of reaction changes from −130333 J to −122247 J for Eqs. (1) and from −32045 J to −27127 J for Eqs. (2) [7]. Reactions Eqs. (1) and (2) are possible.

Probably chemical reaction followed the first SiO_2 formed on the surface of SiC particles during the fabrication of AZ91 matrix composites reinforced by SiC particles and next Mg_2Si formed by reaction Eqs. (1) and Eqs. (2).

Acknowledgements

This work was supported by the Polish Ministry of Science and Higher Education under the grant No. N507 446634 (AGH No. 18.18.170.325) and The European Community for financial support under Marie Curie Transfer of Knowledge grant No. MTKD-CT-2006-042468 (AGH No. 27.27.170.304).

REFERENCE

1. B. Beausir, S. Biswas, D. I. Kim, L. S. Toth, S. Suwas: Analysis of microstructure and texture evolution in pure magnesium during symmetric and asymmetric rolling. Acta Materialia xxx (2009) xxx–xxx.
2. Z. Trojanová, V. Gärtnerová, A. Jäger, A. Námešny, M. Chalupová b, P. Palcek, P. Lukác: Mechanical and fracture properties of an AZ91 Magnesium alloy reinforced by Si and SiC particles. Composites Science and Technology 69 (2009), pp 2256–2264.

3. A. Kleine, J. Hemptenmacher, H. J. Dudek, K. U. Kainer, G. Kroger: Interface formation in carbon fibre reinforced magnesium alloys (AZ91). Journal of Materials Science Letters 14 (1995), pp 358-360.
4. Y. Pan, X. Liu, H. Yang: Microstructural formation in a hypereutectic Mg–Si alloy (Mg_2Si_2). Materials Characterization 55 (2005), pp 241 – 247.
5. Y. Cai, M.J. Tan, G.J. Shen, H.Q. Su: Microstructure and heterogeneous nucleation phenomena in cast SiC particles reinforced magnesium composite. Materials Science and Engineering A282 (2000), pp 232–239.
6. R. D. Schueller, F. E. Wawner, A. K. Sachdev: Nucleation mechanism of the cubic a phase in squeeze-cast aluminium matrix composites. Journal of Materials Science 29 (1994), pp 424 - 435.
7. H. Chen, J. Liu, W. Huang: Corrosion behavior of silicon nitride bonding silicon carbide in molten magnesium and AZ91 magnesium alloy. Materials Science and Engineering A 415 (2006), pp 291–296.